APMIR: An Airborne Polarimeter Designed for High Accuracy

Justin P. Bobak**	Norman R. McGlothlin	David J. Dowgiallo*
Brian C. Hicks	Steven R. Quinn	Troy E. vonRentzell
Louis A. Rose		

Naval Research Laboratory
4555 Overlook Ave.
Washington, D.C. 20375 USA
justin.bobak@nrl.navy.mil

Praxis, Inc.
401 Mill Rd., 5th floor
Alexandria, VA 22314 USA

Interferometrics Inc.
14120 Parke Long Ct.
Chantilly, VA 20151 USA
dave.dowgiallo@nrl.navy.mil

*Corresponding author, **Principal Investigator

Abstract- **The Airborne Polarimetric Microwave Imaging Radiometer (APMIR) has been developed at the Naval Research Laboratory. This instrument was designed primarily as a calibration tool for satellite sensors. As such, the system design began with a challenging error budget. The design and construction followed from the error budget. The system has flown several times. This paper focuses on the design of the instrument and preliminary results.**

I. INTRODUCTION

APMIR has been built to provide calibration and validation (cal/val) data for two satellite programs, as well as for supporting algorithm development. The first satellite is the Defense Meteorological Satellite Program's Special Sensor Microwave Imager Sounder (SSMIS). This satellite has a suite of radiometers, among which are those channels shown in Table 1. All channels provide imaging data that will be used to retrieve ocean wind speed, sea ice properties, land surface properties, water vapor, cloud liquid, and rain rate.

The second program is the Coriolis Windsat, a joint Navy, National Polar-orbiting Operational Environmental Satellite System, and Air Force mission [1]. The satellite was launched in January 2003. It carries five radiometers, three of which are fully polarimetric. Its main objective is to study the polarimetric signature of wind speed and direction over the open ocean. See Table 1 for APMIR, SSMIS, and WindSat frequencies.

The instruments that APMIR will underfly have different characteristics, and require different data sets from the APMIR sensors. This has led to APMIR being developed in stages. The system currently includes channels from 6.6 to 37.0 GHz. Each of these channels provides vertical and horizontal polarization data, and several that are fully polarimetric.

The system is able to scan through a full 360 degrees in azimuth, and the elevation control allows views from nadir to inside the bomb bay (for viewing external calibration targets) of the aircraft. This elevation motion allows for viewing the earth's surface at incidence angles that range

TABLE I
APMIR CHANNEL CAPABILITIES

Frequency (GHz)	Polarization	Matching satellite	Notes
6.6	T_V, T_H	None	Feature
6.8	T_V, T_H	WindSat	
7.2	T_V, T_H	None	Feature
10.7	T_V, T_H, T_3, T_4	WindSat	
18.7	T_V, T_H, T_3, T_4	WindSat	Switchable
19.35	T_V, T_H, T_3, T_4	SSMIS	Switchable
22.235	T_V, T_H	SSMIS	Switchable
23.8	T_V, T_H	WindSat	Switchable
37.0	T_V, T_H, T_3, T_4	SSMIS, WindSat	

from 0 to 60 degrees. APMIR is mounted on a science pallet in the bomb bay of a Lockheed P3 Orion. The aircraft flights have typically been at an altitude of 7.6 km (25 000 ft), and a speed of 270 knots.

The satellite sensors are required to have very high accuracies and sensitivities. Many of the signatures of interest are extremely sensitive to view angle, so pointing knowledge and control is critical to achieving the necessary level of performance. The tight specifications on the satellite instruments correspondingly lead to even tighter error budgets for those sensors utilized for calibration and validation. Table 2 shows the radiometer design specifications for APMIR.

For each of these programs, a comprehensive calibration and validation program is planned. Each of these plans includes data from airborne, ground-based, and satellite-borne instrumentation. Airborne sensors are expected to play a key role in this cal/val effort because by underflying the satellite instrument in question, data from a similar instrument, coincident in both space and time, can be collected. This data is most directly related to that taken by the satellite because it is downward-looking, at corresponding incidence angle and direction, and can encompass the majority of atmospheric and surface effects.

Report Documentation Page

Form Approved
OMB No. 0704-0188

1. REPORT DATE	2. REPORT TYPE	3. DATES COVERED
01 SEP 2003	**N/A**	**-**

4. TITLE AND SUBTITLE	
APMIR: An Airborne Polarimeter Designed for High Accuracy	5a. CONTRACT NUMBER
	5b. GRANT NUMBER
	5c. PROGRAM ELEMENT NUMBER
6. AUTHOR(S)	5d. PROJECT NUMBER
	5e. TASK NUMBER
	5f. WORK UNIT NUMBER
7. PERFORMING ORGANIZATION NAME(S) AND ADDRESS(ES) **Naval Research Laboratory 4555 Overlook Ave. Washington, D.C. 20375 USA**	8. PERFORMING ORGANIZATION REPORT NUMBER
9. SPONSORING/MONITORING AGENCY NAME(S) AND ADDRESS(ES)	10. SPONSOR/MONITOR'S ACRONYM(S)
	11. SPONSOR/MONITOR'S REPORT NUMBER(S)

12. DISTRIBUTION/AVAILABILITY STATEMENT
Approved for public release, distribution unlimited

13. SUPPLEMENTARY NOTES
See also ADM002146. Oceans 2003 MTS/IEEE Conference. Held in San Diego, California on September 22-26, 2003. U.S. Government or Federal Purpose Rights License, The original document contains color images.

14. ABSTRACT

15. SUBJECT TERMS

16. SECURITY CLASSIFICATION OF:			17. LIMITATION OF ABSTRACT	18. NUMBER OF PAGES	19a. NAME OF RESPONSIBLE PERSON
a. REPORT	b. ABSTRACT	c. THIS PAGE			
unclassified	**unclassified**	**unclassified**	**UU**	**6**	

Standard Form 298 (Rev. 8-98)
Prescribed by ANSI Std Z39-18

TABLE II
RADIOMETER SPECIFICATIONS

Frequency (GHz)	Bandwidth (MHz)	NEDT[a] (K)	Beamwidth[b] (degrees)
6.8, 6.6, 7.2	125	0.2	9.4
10.7	300	0.15	5.9
18.7, 19.35	750	0.15	6.8
23.8, 22.23	500	0.2	5.3
37.0	2000	0.1	6.0

[a]Based on an integration time of 0.1 s.
[b]When more than one frequency is listed, the beamwidth presented corresponds to the first of the listed frequencies.

II. SYSTEM REQUIREMENTS

At the time that calibration and validation planning for these missions started, there were several main requirements for an underflight instrument.

First, an imaging system capable of producing a large unobstructed swath was needed for timely coverage and to provide data appropriate for wind direction algorithms that rely on having two looks separated by 180 degrees in azimuth. The necessity for two looks at the same pixel in order to better estimate wind speed is still an open question, and the capability to get appropriate data was considered to be key.

Second, a fully-polarimetric system was needed. The WindSat radiometers provide data at all four Stokes parameters, and a cal/val tool with similar capabilities was needed.

Third, as mentioned in Section I, the satellite instruments have extremely tight error budgets. The error budget for the cal/val system was similarly challenging, and certain parameters were of utmost concern. A system designed with the premise of being a dedicated calibration tool for these two instruments was thought to have the best chance of achieving the necessary level of performance.

APMIR provides 360 degree azimuth swaths and has a large range of unobstructed incidence angle. The data at 10.7, 18.7 or 19.35, and 37.0 GHz is fully polarimetric. Both the electrical and mechanical design have been directed toward achieving the necessary level of accuracy.

Based on a comprehensive analysis of the needed accuracy, an overall error budget for APMIR was constructed. The design proceeded from a comprehensive error budget in order to have the best chance of meeting the needed error levels. In many cases, had more conventional designs been followed, the resulting errors would have been much too large, and this would not have been realized in time to correct the problem.

Commercially available products, or products with a bare minimum of modifications were used whenever possible. However, it proved necessary to have several completely custom pieces designed and built for this project, and some of these will be outlined.

III. SYSTEM DESIGN

A. Mechanical Structure

The system is housed in an aluminum sphere with a diameter of 91.4 cm (36 in). The weight of the sphere, including the internal electronics, is approximately 136 kg (300 lbs). The sphere provides elevation motion and is mounted in a yoke that allows azimuth motion and the second degree of freedom. The yoke structure is constructed using a stressed skin design, resulting in an elevation that is a lightweight laminated aluminum structure. Space inside the vertical portions of the yoke is maximized and provides ample room to mount all elevation drive and braking components. Bridging the two vertical yoke arms is an ultra lightened aluminum structural element that provides attachment surfaces for the vertical elements and a simple interface to the azimuth drive system. Mounting of the sphere to the turret required truncating each side of the shell and attaching a lightened disc element in both openings, completing the enclosure of the radiometers. In addition to providing an interface between the ball and the elevation drive system, the radiometer mounting rack also attaches to these discs creating a concise focal element for combining inertial and air load paths from the sphere. There are two external calibration targets mounted above the sphere on the yoke. The yoke is mounted in the bomb bay of the P3. Fig. 1 shows the internal structure of the sphere, yoke, and science pallet.

Inside the sphere is a rack constructed of extruded aluminum components. The rack was designed to be extremely rigid in order to minimize radiometer antenna movements due to flexure. This rack supports the radiometers and maintains their position. There are three radiometer boxes. Each box contains one or more complete radiometers, including the antenna, RF components, video circuitry, analog-to-digital converter, and microcontroller unit. One box contains the 37 GHz radiometer. A second box houses the 18.7 / 19.35 GHz and 22.235 / 23.8 GHz radiometers. The 6.8 GHz and 10.7 GHz systems are in the last box. A fourth box contains DC-to-DC power converters that accept power at 28V DC and filter and convert it to a variety of different voltage levels needed by the radiometer components.

The antennas are corrugated horns with rexolite lenses. The two sensors that will be underflown have similar but different center frequencies and bandwidths. Due to space considerations, the SSMIS frequencies of 19.35 and 22.235 GHz were combined in one K-band horn, while a second horn, externally identical to the first, was tuned for the WindSat frequencies of 18.7 and 23.8 GHz. The horns are recessed into the sphere in order to maintain the profile for stable airflow. The tunnels formed by recessing the antennas are filled with a closed-cell low-loss foam. It is used to maintain the spherical profile, and it also provides thermal insulation for the antennas. The openings in the sphere were made as large as possible to minimize the degradation of the antenna patterns.

B. Motion Control

Azimuth motion is accomplished using a brushless DC gearhead motor attached to a sprocket and roller chain

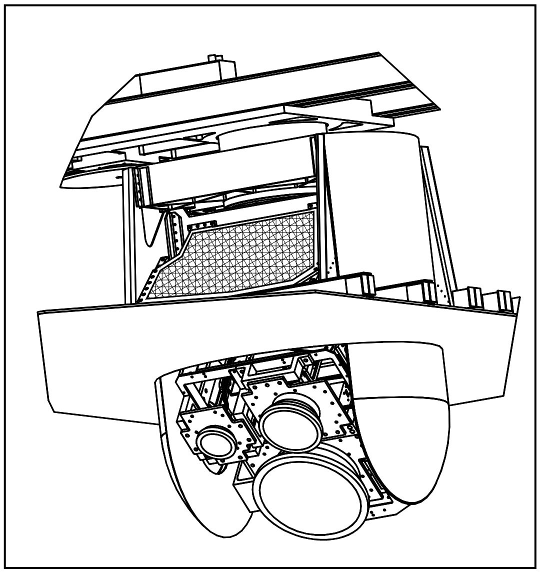

Fig. 1. APMIR mounting configuration

transmission, resulting in a 105:1 reduction. The azimuth drive components are protected by an adjustable torque limiting clutch which will slip in cases of extreme accelerations.

Elevation motion is accomplished by a combination of “commercial off the shelf” hardware and custom designed components. Elevation motion of the sphere is via a brushless DC gearhead motor driving a custom worm gear attached to the elevation spindle. An electrically-operated clutch is inline between the motor and worm gear. A 640:1 speed reduction is obtained from the pairing of the planetary gear set at the motor and the worm drive at the spindle. An elevation brake is built into the system to eliminate the positional jitter that could result from the backlash inherent in the elevation drive. This is an electro-mechanically actuated disc brake system that utilizes a magnetic particle clutch to provide a constant torque to a miniature ball screw that delivers an evenly applied force to the brake caliper. Data taking will typically only occur while the elevation brake is engaged. During takeoff and landing of the aircraft, the sensor is placed in a stowed position (with horns pointed into the bomb bay) to reduce damage from debris during these intervals.

The angular position of the sphere in relation to the aircraft is measured by 16-bit 32x resolvers. The angular accuracy in each degree of freedom is 0.012 degree. The resolvers are run in an incremental rather than absolute mode, with absolute position determined from mechanical position switches on each axis of rotation.

Typically, the sphere will rotate in the azimuth direction at 12 rpm for imaging (with 53° incidence angle, altitude of 25000 ft and aircraft speed of 270 kts). Every few minutes, the sphere will rotate in elevation to view the external calibration targets. The two calibration loads require a total of four unique look angles to allow the three horns to view the calibration targets at nearly perpendicular incidence angles. The mounting of the targets on the yoke is such that the targets are within the bomb bay of the aircraft. The sphere can continue its azimuth motion while it looks at the targets, as these rotate with the sphere. This reduces wear on the azimuth drive components, and reduces scene data loss during external calibration periods.

IV. ELECTRICAL SYSTEMS

A. Radiometers

Each radiometer is designed in a similar fashion. Separate RF chains are used for the vertically and horizontally-polarized signals. This topology was chosen both to reduce data loss due to single point failure and to simplify troubleshooting. The radiometers follow a total power radiometer design to maximize sensitivity, and use direct detection to avoid problems with oscillators, such as temperature drift and VSWR problems. Isolators are used liberally to control reflections. The fully-polarimetric sensors employ polarization combining to form the +45- and –45-degree and left- and right-circular polarizations (LCP and RCP). The differences between each pair will be calculated in processing to form the third and fourth Stokes parameters [2]. Polarization combining was chosen over correlation due to concerns over proper calibration of correlators. The combining occurs in custom-made modules that each have two inputs (vertical and horizontal polarizations) and six outputs to which the tunnel diode detectors are directly attached.

Each detector output is measured across a load resistor uniquely chosen to maximize linearity for that particular detector. The choice of the optimal resistance values arose from the results of a two-tone test [3] performed on the detectors. The detectors for signals that were to be combined in post processing were also matched with each other according to the results of the two-tone test.

The video section, termed the Radiometer Control Module (RCM) is an integrated unit containing all of the hardware necessary for radiometer control and data acquisition. It was designed and constructed by the Remote Sensing Division. Every aspect of the observing process is dynamically reconfigurable via an on-board 16-bit 68HC12 based microcontroller unit (MCU).

Acquisition of science data is accomplished through eight identical analog-to-digital conversion modules (ADCM). Six of the channels are dedicated to simultaneously sampling six parameters (V, H, +45, -45, RCP, LCP) of a given radiometer and the remaining two channels are used for monitoring platinum resistance thermometers (PRTs) and inclinometers (measuring the attitude of the horns). Each ADCM consists of a high precision, low noise instrumentation amplifier, a programmable gain stage, a programmable offset control, a programmable 2-pole analog anti-aliasing filter, and a 16-bit analog-to-digital converter (ADC) with an internal track-and-hold. The outputs of the ADCs are sampled

approximately every 50 milliseconds. Great attention to detail was exercised in the design of the ADCM; all bias voltages were derived from the same internal precision voltage reference used for a specific ADC, signal and power lines were routed orthogonally, and ground planes were isolated and carefully split to inhibit eddy currents.

Control of pin-switches and latching circulators required for radiometer calibration is accomplished by a digital subsystem of the RCM providing 16 buffered TTL outputs and 8 outputs which can each be configured as either open collector outputs (100 mA sink capability) or as additional TTL outputs. All outputs transition simultaneously under the direct control of the MCU to facilitate a variety of calibration algorithms which can be selected via the host computer.

The RCM also incorporates a transformer-isolated RS422 interface to receive commands and transmit science data to a host computer. The RCM is housed in a metal enclosure that is 4 cm x 9.5 cm x 10.2 cm (1.56 in. x 3.75 in. x 4.0 in.).

B. *Calibration*

Both internal and external calibration sources are utilized. As mentioned above, there are two external calibration loads. One of these is heated to about 40°C, while the other is at ambient bomb bay air temperature. Each target is an octagonal aluminum substrate (45.7 cm x 51.4 cm or 18” x 20.25”) into which pyramids have been formed by spark erosion. Each octagon is formed from four separately formed sections due to the size of the overall target. Thermally-conductive material has been placed at the interfaces of each section to minimize thermal gradients. The pyramids have a 4:1 height-to-width ratio and are coated with a 1.5 mm layer of silicone-based absorber. The silicone material was chosen over epoxy-based materials because of its relatively high tolerance to thermal stress. The coating thickness was chosen as a compromise between thermal gradients and emissivity. A thicker coating would have a higher emissivity (particularly at the lower frequencies), but would be subject to much larger temperature gradients from back to front. A thinner coating would have better physical temperature performance at the cost of reduced emissivity. In order to avoid condensation (if the ambient target is cooled in the future) and also to minimize thermal gradients arising from convection, a layer of foam (the same used over the antennas) is placed over the pyramids.

Temperature sensors are embedded in the aluminum substrate and in the absorbing coating to monitor the temperature of the targets. The sensors are four-wire PRTs. Twenty-four are mounted in each target, and these were placed to measure gradients both across the face of the target and within the absorbing coating itself. Substantial gradients have been found across the depth of the absorber on similar targets [4], and the PRTs in the tips of the pyramids and in the valleys between pyramids will allow better characterization of these gradients.

The internal calibration currently consists of ambient terminations and noise diodes biased by custom designed high-precision constant current sources. The constant current source circuits have been designed with components that minimize thermal variations. A fully-polarimetric calibration system has been designed at NRL, and recently put into place. The design and results from testing this calibration system will be discussed in a future paper.

C. *Software*

The architecture of the control software is a foreground, background process control system. The foreground process handles the user interface to configure the system, control data acquisition, and provide visual feedback to the operator about the quality of the data being acquired. The user can configure and observe the raw communication to and from each radiometer, configure and control a selectable radiometer, view current data (both text and historic graphic plots), develop data acquisition control scripts for each radiometer, control the orientation and spin rate of the sphere, and control the storage of data. Provision for real time imagery has now been developed. The background process handles the communication and data storage activities via twelve interrupt driven communication routines, each multi-threaded.

V. ANTENNA POINTING

Accurate and precise knowledge of antenna pointing is critical to maintaining the error budget. There is a strong dependence of ocean surface brightness temperature on incidence angle [5]. Additionally, since the difference between vertically- and horizontally-polarized brightness temperature is large, a small amount of uncorrected polarization mixing due to antenna roll produces a large error. The three angles that characterize the antenna pointing are the Earth Incidence Angle (EIA), Polarization Rotation Angle (PRA), and Scan Azimuth Angle (SAA). These angles correspond in a similar manner to the radiometer pitch, roll, and yaw, respectively.

Earth Incidence Angle is the incidence angle of the antenna beam with respect to the normal to the surface. For incidence angles around 53° (used for SSM/I, SSMIS, and WindSat), the brightness temperature of the ocean surface can change by about 2 Kelvin per degree of angle.

Polarization Rotation Angle is a roll angle of the horn about its boresight axis. It results in polarization mixing as a portion of the vertically-polarized signal is coupled by the horn and OMT into the horizontal polarization signal chain and horizontally-polarized signal is coupled into the vertical polarization signal chain. Since the vertically- and horizontally-polarized brightness temperatures can differ by over 100 K over the ocean at incidence angles near 53°, a small uncertainty in PRA can cause a large uncertainty in brightness temperature.

Scan Azimuth Angle is the true compass direction of radiometer pointing. This angle is important because of the azimuthal dependence of the wind direction signal over the ocean.

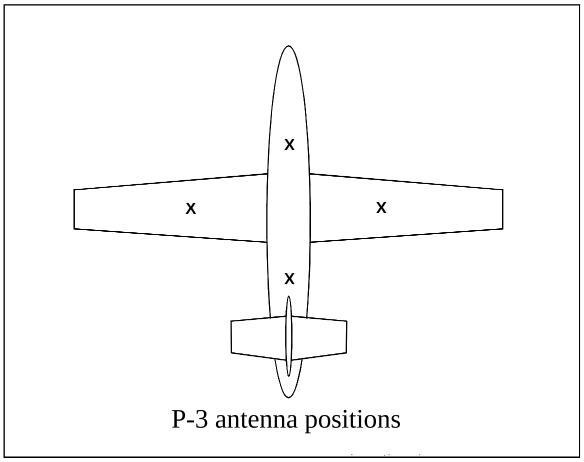

Fig. 2. GPS antenna mounting

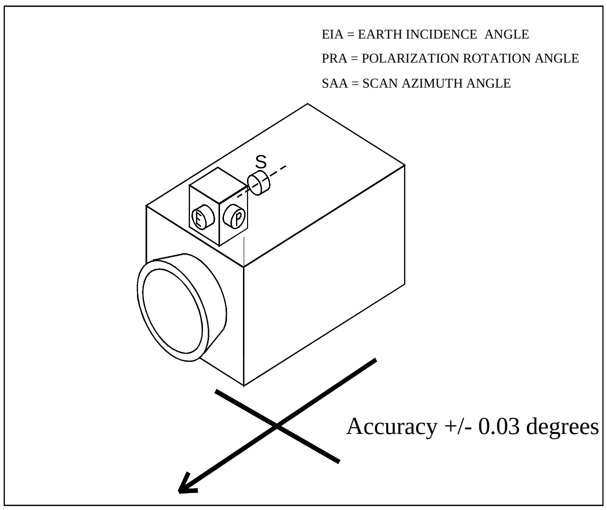

Fig. 3. Inclinometer mounting

In order to measure these angles with sufficient accuracy, a multi-layer system is used. Each horn has a set of three inclinometers permanently mounted on it to measure the key angles as shown in Figure 3. Each inclinometer was calibrated after attachment to the horn by a laser alignment procedure in which the gain and offset of the inclinometers were calibrated to within hundredths of a degree. When the antennas were taken to the anechoic chamber for measurements, the inclinometers were used to tie the measured antenna patterns back to absolute gravity. In this way, the patterns can be tied to gravity upon installation of the sensors on the aircraft.

The inclinometers, as gravity-based sensors, will not provide reliable data in flight when they are subjected to centrifugal forces. To overcome this, during installation, the inclinometer data is mapped to the resolvers of the gimbaled system. These sensors monitor the position of the sphere with respect to the aircraft. The last stage is to monitor the attitude of the aircraft with respect to the earth, which is accomplished by a GPS-based position and attitude determination system, the Trimble Navigation TANS Vector. Through the appropriate transformations [6], the antenna pattern measurements taken at the antenna range can be mapped onto the scene. For aircraft attitude redundancy, a laser ring gyroscope system is mounted in the cabin of the aircraft and this data is recorded during flight. Four GPS antennas are mounted on the aircraft, as shown in Fig. 2, in order to derive the attitude to an accuracy of +/- 0.08 degrees.

VI. ENVIRONMENTAL CONTROLS

Providing the radiometers with the most stable operating environment possible is an important component of maintaining the error budget, despite all of the effort that has gone into making the system tolerant of nonoptimal surroundings. The considerations include thermal control, power supply filtering, and electromagnetic interference suppression.

A. Thermal control

During the design of APMIR, limits were set on the temperature set point repeatability and the acceptable rate of temperature drift. A temperature controller was designed in the Remote Sensing Division to meet these specifications. It utilizes proportional control rather than hard on-off cycling in order to minimize either temperature or power supply ripples arising from heater switching. The heaters are cartridge heaters embedded in the radiometer baseplates. The radiometer enclosures are each protected by thermal blankets. To ensure that the sensors will achieve desired temperatures within a desired time even after being cold-soaked, a system for preheating before flight has also been designed.

The physical temperatures inside each radiometer and on the external targets are monitored by various grades of 100 ohm PRTs. Each PRT is sampled individually by use of a multiplexer ("mux") circuit designed and built in the Remote Sensing Division. The mux board is separated into four identical sections. Each section has a constant current source driving a 2mA current through four impedances (two PRTs and two precision fixed resistors of known value) connected in series. A 2-bit multiplexer in each section provides differential voltage measurements across any of four distinct impedances. The fixed resistors allow a continual two-point calibration of that section. Before leaving the multiplexer board, the differential voltage is amplified via an instrumentation amplifier and a DC offset is added to align the signal to a corresponding temperature window. The signal is then sent to the RCM for further processing and digitizing.

B. Power supply conditioning

Conditioning the bias voltages has been a concern. Power on the aircraft is inherently noisy, and the noise is increased by running the power through slip rings. A multilayer filtering approach has been used. Aircraft power that is destined for the radiometer electronics power is converted from 60Hz, 120 VAC to 28 VDC by a linear power supply in the aircraft cabin, providing very clean power. After being transmitted from the linear power

supply through the slip rings and into the sphere, the power is sent to the sphere power module (SPM). In the SPM, a number of switching DC-to-DC power supplies convert the 28 VDC to all of the needed bias levels for the radiometers. Additionally, these power supplies eliminate some of the potential ground loops in the system. Each supply is heavily filtered at the input and output, reducing the ripple to 5 mV or less. This power is then sent to the radiometer enclosures, where it is further filtered as necessary.

C. ElectromagneticInterference (EMI) suppression

Each radiometer enclosure and the SPM have EMI gasketing at all joints. To minimize errors after digitization within the radiometer, data is sent back to the controlling pc within the aircraft cabin via RS422, a differential communications protocol. The differential signals are run through twisted pair cables wherever possible.

VII. STATUS AND FUTURE PLANS

The APMIR system is currently underflying the WindSat satellite as part of the calibration and validation effort. Sample data is shown in Figure 4. Geolocation results have been good and preliminary uncorrected brightness temperature comparisons with SSM/I data have been promising.

Additional WindSat underflights are scheduled for Fall of 2003. These may occur in conjunction with SSMIS underflights.

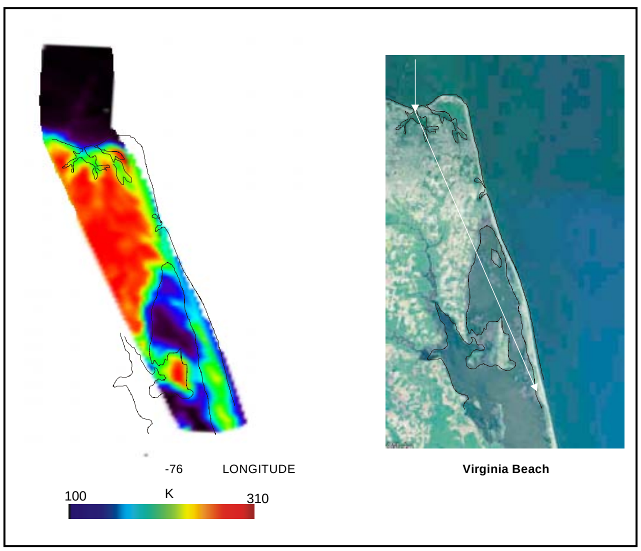

Fig. 4. APMIR 18 GHz horizontal polarization, coastal flight of Virginia Beach, VA.

Note: Flight path shown on visible map at right. Coast line highlighted for contrast.

VIII. ACKNOWLEDGMENTS

This work has been funded by the Office of Naval Research, the Defense Meteorological Satellite Program's SPO, and the NPOESS Integrated Program Office.

IX. References

[1] K. St.Germain and P. Gaiser, "Spaceborne polarimetric microwave radiometry and the Coriolis WindSat system," *2000 IEEE Aerospace Conference Proceedings CD-ROM*.

[2] P. Gaiser, P. Chang, and L. Li, "Ocean surface wind direction retrievals using microwave polarimetric radiometer data," *Proceedings of the 1996 International Geoscience and Remote Sensing Symposium*, vol. II, pp. 1123-1125.

[3] V. Reinhardt, Y. Shih, P. Toth, S. Reynolds, and A. Berman, "Methods for measuring the power linearity of microwave detectors for radiometric applications," *IEEE Transactions on Microwave Theory and Techniques*, vol. 43, no. 4, pp. 715-720, April 1995.

[4] McGrath, A. and T. Hewison, "Measuring the accuracy of MARSS – an airborne microwave radiometer," *Journal of Atmospheric and Oceanic Technology*, vol. 18, no. 12, pp. 2003-2012, December 2001.

[5] Yueh, S., "Modeling of wind direction signals in polarimetric sea surface brightness temperatures," *Transactions on Geoscience and Remote Sensing*, vol. 35, no. 6, pp. 1400-1418, November 1997.

[6] J. Piepmeier, "Remote sensing of ocean wind vectors by passive microwave polarimetry," Ph.D. dissertation, Georgia Institute of Technology, pp. 61-73, July 1999.